# The thermotropic phase behavior of cationic lipids: calorimetric, infrared spectroscopic and X-ray diffraction studies of lipid bilayer membranes composed of 1,2-di-O-myristoyl-3-N...

**ARTICLE** *in* BIOCHIMICA ET BIOPHYSICA ACTA · MARCH 2001

Impact Factor: 4.66 · DOI: 10.1016/S0005-2736(00)00336-9 · Source: PubMed



**4 AUTHORS**, INCLUDING:

Stephanie Tristram-Nagle
Carnegie Mellon University
**111** PUBLICATIONS **7,583** CITATIONS
SEE PROFILE

John F Nagle
Carnegie Mellon University
**210** PUBLICATIONS **12,512** CITATIONS
SEE PROFILE

ELSEVIER

Biochimica et Biophysica Acta 1510 (2001) 70–82

BIOCHIMICA ET BIOPHYSICA ACTA
BBA

www.elsevier.com/locate/bba

# The thermotropic phase behavior of cationic lipids: calorimetric, infrared spectroscopic and X-ray diffraction studies of lipid bilayer membranes composed of 1,2-di-*O*-myristoyl-3-*N,N,N*-trimethylaminopropane (DM-TAP)

Ruthven N.A.H. Lewis [a], Stephanie Tristram-Nagle [b], John F. Nagle [b,c], Ronald N. McElhaney [a,*]

[a] *Department of Biochemistry, University of Alberta, Edmonton, Alta., Canada T6G 2H7*
[b] *Department of Biological Sciences, Carnegie Mellon University, Pittsburgh, PA 15213, USA*
[c] *Department of Physics, Carnegie Mellon University, Pittsburgh, PA 15213, USA*

Received 13 April 2000; received in revised form 31 August 2000; accepted 14 September 2000

**Abstract**

The thermotropic phase behavior of lipid bilayer model membranes composed of the cationic lipid 1,2-di-*O*-myristoyl-3-*N,N,N*-trimethylaminopropane (DM-TAP) was examined by differential scanning calorimetry, infrared spectroscopy and X-ray diffraction. Aqueous dispersions of this lipid exhibit a highly energetic endothermic transition at 38.4°C upon heating and two exothermic transitions between 20 and 30°C upon cooling. These transitions are accompanied by enthalpy changes that are considerably greater than normally observed with typical gel/liquid–crystalline phase transitions and have been assigned to interconversions between lamellar crystalline and lamellar liquid–crystalline forms of this lipid. Both infrared spectroscopy and X-ray diffraction indicate that the lamellar crystalline phase is a highly ordered, substantially dehydrated structure in which the hydrocarbon chains are essentially immobilized in a distorted orthorhombic subcell. Upon heating to temperatures near 38.4°C, this structure converts to a liquid–crystalline phase in which there is excessive swelling of the aqueous interlamellar spaces owing to charge repulsion between, and undulations of, the positively charged lipid surfaces. The polar/apolar interfaces of liquid–crystalline DM-TAP bilayers are not as well hydrated as those formed by other classes of phospho- and glycolipids. Such differences are attributed to the relatively small size of the polar headgroup and its limited capacity for interaction with moieties in the bilayer polar/apolar interface. 

*Keywords:* Lipid bilayer membrane; Polymorphic phase behavior; Cationic lipid; 1,2-Di-*O*-myristoyl-3-*N,N,N*-trimethylaminopropane; Differential scanning calorimetry; Infrared spectroscopy; X-ray diffraction

Abbreviations: DM-TAP, 1,2-di-*O*-myristoyl-3-*N,N,N*-trimethylaminopropane; DNA, deoxyribonucleic acid; FTIR, Fourier-transform infrared; DSC, differential scanning calorimetry; $CH_2$, methylene; C=O, carbonyl; $T_m$, hydrocarbon chain-melting phase transition temperature; $L_\alpha$, lamellar liquid–crystalline; $L_\beta$, lamellar gel; $L_c$, lamellar crystalline; CHESS, Cornell high energy synchrotron source

* Corresponding author. Fax: +1-780-492-0095; E-mail: rmcelhan@gpu.srv.ualberta.ca

0005-2736/01/$ – see front matter 
PII: S0005-2736(00)00336-9

## 1. Introduction

The physical properties of lipid assemblies which contain or are composed entirely of cationic lipid molecules are of considerable practical and fundamental interest. Cationic lipids have been utilized as detergents and for the formation of fairly robust model membranes ([1–10] and references cited therein), and some effort has even been expended in using cationic lipid membranes to develop reaction-specific surface catalysts [8,11,12]. Double-chained cationic amphiphiles have also been investigated as potential antimicrobial agents and some of the short chain derivatives of these materials have proven to be fairly effective in this regard [13]. These materials have also been investigated as potential anti-inflammatory agents [14].

Recently, considerable effort has been invested in the development of cationic amphiphiles in general, and double-chained cationic amphiphiles in particular, as potential deoxyribonucleic acid (DNA) transfection agents [15–21]. This particular application is based on the fact that the positively charged polar headgroups of these lipids bind very strongly to negatively charged DNA to form a lipid–DNA complex which may be sufficiently lipophilic to traverse cell membranes [15]. To date, much effort has been expended in the characterization of cationic lipid complexes with DNA [22–28], in the assay of their DNA transfection efficiency [29,30], and in development of structure–function relationships [16,29,31–33]. Currently there is no clear consensus on the relationship between DNA transfection efficiency and cationic amphiphile structure, although there are indications that transfection efficiency may be affected by small changes in the overall hydrophile–lipophile balance of the cationic lipid molecule [20,29,32,33], as well as the capacity of the lipid–DNA complex to form inverted non-lamellar phases [25,29]. The relationship between the structure of cationic lipids and their efficiency as DNA transfection agents is currently under active investigation in several laboratories and a clearer consensus on this topic may emerge soon.

Despite considerable interest in the properties of cationic lipids and their derived membranes, our current knowledge of the structure and organization of membranes composed of pure cationic lipids is not extensive [1,3,6,8,34–41]. To date, a few differential scanning calorimetry (DSC) studies of the thermotropic phase behavior of some double-chained cationic amphiphiles derived from quaternary ammonium salts have appeared, along with a characterization of their mixtures with various anionic and zwitterionic phospholipids [39,41]. Such studies reveal that the cationic lipids exhibit unusual mixing properties with negatively charged and zwitterionic phospholipids, presumably because of strong interactions between the headgroups of the cationic lipids and the negatively charged phosphate moieties of the phospholipid molecules. It has also been shown that such interactions can markedly affect the conformation of phospholipid headgroups at the surface of the lipid bilayer [42–45] and, depending on the surface charge of the bilayer, such interaction may either accentuate or attenuate membrane non-lamellar phase-forming propensity [46]. Although such studies provide some insight into the structure and organization of cationic lipid membranes, our understanding of this particular area is limited. To fill this void, we have begun to study the thermotropic phase behavior, structure and organization of bilayer model membranes composed of cationic lipids, with initial emphasis on those lipids that have been developed as potential DNA transfection agents. Our studies are also intended to address fundamental issues related to the effect of surface charge on the properties of lipid bilayers and the way in which these effects are influenced by the proximity of such charges to the bilayer polar/apolar interface. In this paper, we present the results of DSC, Fourier-transform infrared (FTIR) spectroscopic and X-ray diffraction studies of cationic lipid membranes composed of 1,2-di-*O*-myristoyl-3-*N,N,N*-trimethylaminopropane (DM-TAP). This lipid belongs to a class of double-chained cationic lipid amphiphiles which show considerable promise as potentially effective DNA transfection agents [26,29,47–50].

## 2. Materials and methods

The lipid DM-TAP was obtained from Avanti Polar Lipids Inc. (Alabaster, AL, USA) and used without further purification. The structure of DM-TAP is shown in Fig. 1. For DSC studies, 3–4 mg of dried

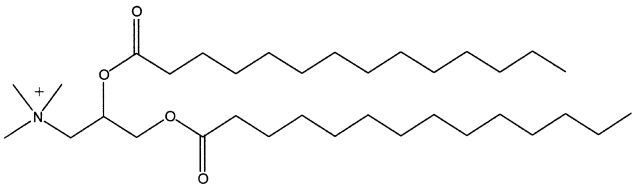

Fig. 1. Diagram illustrating the chemical structure of DM-TAP. The conformation shown in the drawing is for illustrative purposes only and is not intended to make any inferences about the conformation actually adopted by the molecule.

lipid was weighed directly into the hastelloy ampoules of the calorimeter and 0.5 ml of a buffer containing 50 mM sodium phosphate, 100 mM NaCl, 1 mM $NaN_3$, pH 7.4 was added. After sealing the ampoule, the lipid sample was hydrated in situ by three cycles of heating and cooling between −30°C and 60°C at heating rates of 1°C/min. Data were acquired with a high-sensitivity, multi-cell differential scanning calorimeter (Calorimetry Sciences Corporation, Provo, UT, USA) operating at scan rates near 10°C/h. The data acquired were analyzed and plotted using the Origin software package (Microcal Software Inc., Northampton, MA, USA).

For the FTIR spectroscopic experiments, samples were prepared by dispersing 1–2 mg of the lipid sample in 75 μl of a $D_2O$-based sodium phosphate buffer (as above) at temperatures near 60°C. The mixture obtained was squeezed between the $CaF_2$ windows of a heatable, demountable liquid cell (NSG Precision Cells, Farmingdale, NY, USA) equipped with a 25 μM teflon spacer. Once mounted in the sample holder of the spectrometer, the sample could be heated between −20°C and 90°C by an external, computer-controlled water bath. Infrared spectra were acquired as a function of temperature with a Digilab FTS-40 Fourier-transform spectrometer (Bio-Rad, Digilab Division, Cambridge, MA, USA) using data acquisition parameters similar to those described by Mantsch et al. [51]. The experiment involved a sequential series of 2°C temperature ramps with a 20 min inter-ramp delay for thermal equilibration, and was equivalent to a scanning rate of 4°C/h. Data were analyzed using Digilab software and other software from the National Research Council of Canada, and plotted with the Origin software package (Microcal Software Inc., Northampton, MA, USA). In cases where absorption bands appeared to be a summation of components, a combination of Fourier deconvolution and curve fitting procedures was used to obtain estimates of the positions of the component bands and to reconstruct the contours of the original envelope.

X-ray diffraction experiments were performed with both macroscopically oriented and capillary-mounted powder samples. The capillary-mounted samples were prepared as follows: 15 mg of DM-TAP was added to 100 mg of 100 mM potassium phosphate buffer, pH 7.0. The lipid suspension was cycled between 0 and 60°C three times, and then loaded into pre-cleaned X-ray glass capillaries (Charles Supper Co., Cambridge, MA, USA). The capillaries were then loaded into a cassette that was placed in a chamber with thin mylar windows where temperature was controlled to ±0.05°C using a Lake Shore Cryotronics Controller (Westerville, OH, USA). Diffraction measurements were carried out using a 4-circle Huber diffractometer (Blake-Huber, Scotch Plains, NJ, USA) mounted onto a Rigaku fixed tube source (Rigaku USA, Boston, MA, USA) operating at 2.3 kW. The instrumental resolution was obtained with three sets of Huber slits set to 0.5 mm horizontally and 5 mm vertically, and was measured to be 0.02 $Å^{-1}$ in $q$-space. Data were collected using a Phosphor-Imager obtained from Molecular Dynamics (Sunnyvale, CA, USA) and a Bicron scintillation counter (Bicron, Newbury, OH, USA) to check angles. Additional scans were obtained using a Rigaku H3R rotating anode operated at 5.2 kW with the Phosphor-Imager. X-ray exposures of 1–2 h were used with a resolution of $\cong 0.04$ $Å^{-1}$. Oriented samples were prepared using a modified 'rock and roll' procedure [52]. The lipid sample was deposited from a chloroform/methanol (10:1) mixture onto the outside of a 30 ml curved glass beaker and placed in a specially constructed X-ray chamber on loan from Dr. John Katsaras and the Chalk River Laboratories (Chalk River, Ont., Canada) in which full hydration was achieved using water vapor [53]. Once the sample was fully hydrated, it was possible to effect a partial dehydration of the sample by removing the aqueous reservoir from within the inner compartment of the X-ray chamber and leaving the outer compartment unsealed. Under these conditions, sample dehydration occurred over time because of the slow leakage of

water vapor from the X-ray chamber. Oriented samples were examined using the rotating anode generator, and with the higher intensity of a synchrotron source at CHESS (Cornell high energy synchrotron source) (Cornell University, Ithaca, NY, USA). The latter enabled acquisition of higher resolution data (0.002 $Å^{-1}$) which were recorded with a CCD camera [54]. Low- and wide-angle diffraction data were acquired at temperatures bracketing the calorimetrically detected thermotropic events. The positions of the diffraction peaks were used to determine interlamellar $D$ spacings (low-angle measurements) and to calculate unit cell dimensions (wide-angle measurements). Subcell dimensions were determined by methods similar to those described by Maulik et al. [55], but using a unit cell which contains two chains. The angle $\beta$ (see Fig. 9) was determined thus:

$$\cos\beta = d_{20}(d_{11}^{-2} - d_{1\bar{1}}^{-2}) / \sqrt{2d_{11}^{-2} + 2d_{1\bar{1}}^{-2} - d_{20}^{-2}}$$

The unit cell dimensions $a$ and $b$ (see Fig. 9) were determined from the following equations:

$$a = 2d_{20}/\sin\beta$$

$$b = a/\left(d_{20}\sqrt{2d_{11}^{-2} + 2d_{1\bar{1}}^{-2} - d_{20}^{-2}}\right)$$

## 3. Results

### 3.1. DSC

Illustrated in Fig. 2 are the DSC heating and cooling thermograms exhibited by aqueous dispersions of DM-TAP. Upon heating, this lipid exhibits a single sharp, slightly asymmetric endothermic transition centered near 38.4°C, and, upon cooling, two overlapping exothermic peaks are observed at temperatures near 25.2°C and 23.3°C. These phase transitions are highly energetic with total enthalpy values of 15.9 and 13.7 kcal/mol (heating and cooling modes, respectively). We also find that there is a kinetic component to the behavior of DM-TAP which is manifest primarily by scan rate-dependent changes in the cooling exotherms. Thus, with increases in cooling rate, a downward shift in the temperature of the exothermic transitions, a decrease in the enthalpy values measured, and a change in the distribution of the measured enthalpy between the two cooling exothermic peaks are observed. The physical basis of this and other aspects of the thermotropic phase behavior of this lipid were examined by a combination of FTIR spectroscopy and X-ray diffraction (see below).

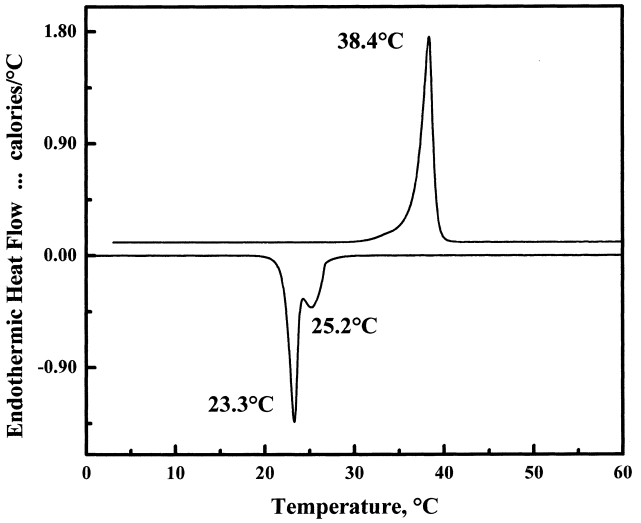


Fig. 2. DSC heating (top) and cooling (bottom) thermograms exhibited by aqueous dispersions of DM-TAP. The data were acquired at scan rates near 10°C/h.

### 3.2. FTIR spectroscopy

Illustrated in Fig. 3 are selected regions of the FTIR spectra of DM-TAP acquired at temperatures below and above the single endothermic transition detected in our DSC heating experiments. The absorption bands observed at temperatures below the $T_m$ (hydrocarbon chain-melting phase transition temperature) are fairly sharp and relatively well resolved from each other, whereas at temperatures above the $T_m$, absorption bands are considerably broader and are not as well resolved. In some regions of the infrared spectrum, these changes are also accompanied by well defined shifts in the observed absorption maxima (for examples, see Fig. 4). These spectral features provide information about the structures of the low- and high-temperature phases of this lipid and about the nature of the interconversion between them ([55] and references cited therein). A description and interpretation of these spectroscopic observations are presented below.

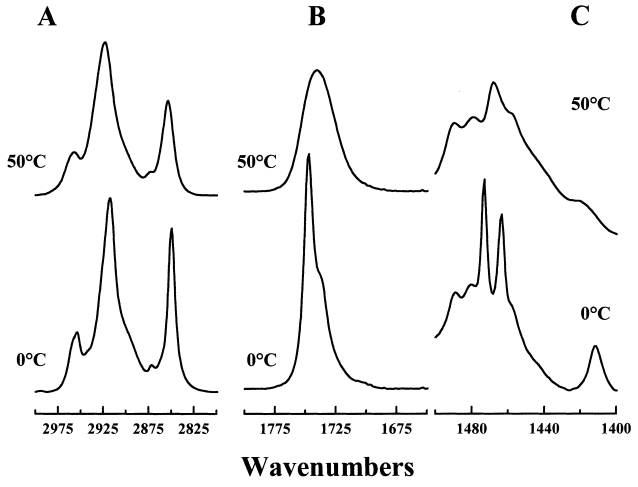


Fig. 3. Representative absorbance spectra showing the contours of the C–H stretching (A), C=O stretching (B) and C–H bending (C) regions of the $L_c$ (0°C) and $L_\alpha$ (50°C) phases of DM-TAP.

The temperature-dependent changes of the maxima of the methylene ($CH_2$) symmetric stretching and $CH_2$ scissoring absorption bands of the infrared spectra of DM-TAP are presented in Fig. 4. These particular spectroscopic markers are sensitive to changes in the conformation and in the lateral packing interactions between hydrocarbon chains, respectively. In the $CH_2$ stretching region of the spectrum (2800–3000 $cm^{-1}$), an abrupt increase in the peak frequencies of the $CH_2$ symmetric (Fig. 4A, solid symbols) and asymmetric stretching band (not shown) occurs when aqueous dispersions of DM-TAP are heated to temperatures above 38°C. This frequency increase is also accompanied by an abrupt increase in the width of the absorption bands over the same temperature range (data not shown). Increases in the frequencies and widths of these absorption bands are indicative of a decrease in hydrocarbon chain conformational order and an increase in overall mobility characteristic of the melting of all-*trans* polymethylene chains ([56] and references cited therein). Upon cooling, the process is fully reversible albeit with a hysteresis of some 7–8°C under our conditions (Fig. 4A, open symbols). However, the observed cooling hysteresis is less pronounced than observed by DSC (≅12–13°C) and only a single thermotropic transition centered near 29°C is observed. The differences in the cooling behavior observed in the DSC and FTIR spectroscopic experiments are probably attributable to greater kinetic distortions caused by the faster effective cooling rate employed in the DSC experiment.

At temperatures below 38°C, the main $CH_2$ scissoring band appears as a well resolved doublet, the components of which are very sharp and centered near 1463 $cm^{-1}$ and 1473 $cm^{-1}$ (see Figs. 3C and 4B). Upon heating, this doublet collapses abruptly to form a single broader band centered near 1468 $cm^{-1}$ at temperatures near the $T_m$ (see Figs. 3C and 4B). Upon cooling, these spectroscopic changes are fully reversed at temperatures near 29°C as observed with the $CH_2$ stretching band. The appearance of the $CH_2$ scissoring band as a well resolved doublet at temperatures just below the $T_m$ is not typical of the lamellar gel ($L_\beta$)-like lipid phases, which usually exhibit a single $CH_2$ scissoring band centered near 1468 $cm^{-1}$ under comparable conditions ([56] and references cited therein). However, such behavior has been observed with lipid lamellar crystalline ($L_c$) phases (for examples, see [58–60]). Our observations therefore suggest that the low-temperature form of DM-TAP is a $L_c$ phase and not the $L_\beta$ gel phase observed with most phospho- and glycolipids. Thus the heating endothermic transition which this lipid exhibits is probably a $L_c$ to lamellar liquid–crystalline ($L_\alpha$) phase transition.

The main $CH_2$ scissoring band near 1468 $cm^{-1}$ is of special significance because it provides information about the modes of hydrocarbon chain packing

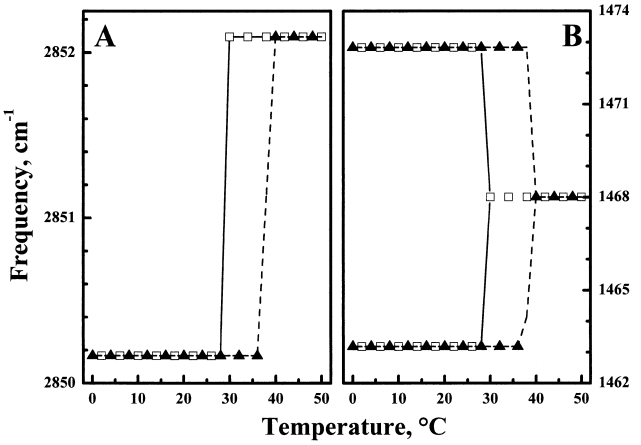


Fig. 4. Temperature dependence of the band maxima of the $CH_2$ symmetric stretching (A) and $CH_2$ scissoring absorptions (B) observed upon heating (— —▲— —) and cooling (–□–).

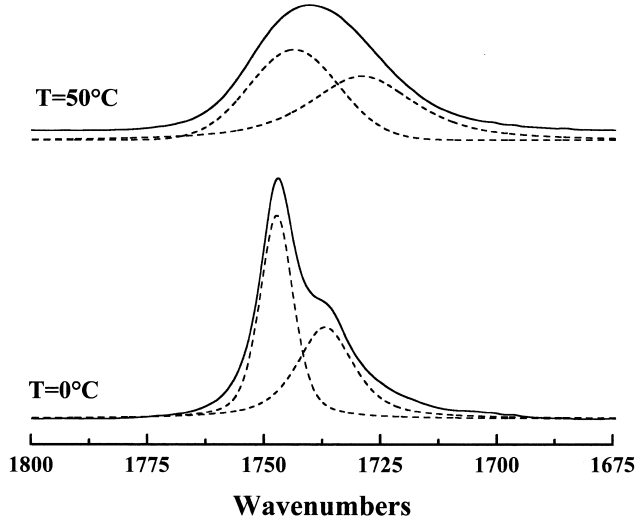


Fig. 5. Fine structure of the C=O stretching absorption bands of the crystalline (0°C) and liquid–crystalline (50°C) phases of DM-TAP. Spectra are presented in the absorbance mode with the solid lines representing the contours of the acquired absorption bands and the dashed lines representing the component bands estimated by a combination of Fourier deconvolution and curve fitting. The component bands are drawn to a baseline offset from that of the 'real' spectra.

[56]. The band splitting (also called crystal-field splitting, factor-group splitting, or correlation-field splitting) observed at low temperature has been correlated with a coupling of the scissoring vibrations of inequivalent all-*trans* polymethylene chains that are arranged in subcells with their zigzag planes perpendicular to each other [60,61]. The collapse of this splitting at higher temperatures can thus be attributed to the uncoupling of these interactions coincident with the formation of a more loosely packed structure in which the hydrocarbon chains are rotationally disordered [57]. A more detailed analysis of this aspect of our FTIR spectroscopic observations will be presented in Section 4.

The C=O stretching region of the infrared spectrum of this lipid contains a strong absorption band arising from the two carbonyl groups of the acyl chains of the molecule. At temperatures above the $T_m$, DM-TAP exhibits a fairly broad C=O stretching absorption band which appears to be a summation of components centered near 1743 $cm^{-1}$ and 1728 $cm^{-1}$ (see Fig. 5), frequencies comparable to those normally observed in the $L_\alpha$ phase of bilayers composed of phospho- and glyco-glycerolipids (for examples, see [58,59,62–64]). These two components result from differential infrared absorption by populations of 'free' and hydrogen-bonded ester carbonyl groups, respectively [65,66]. Given that interfacial water is the sole source of hydrogen-bonding donor groups present in DM-TAP membranes, we conclude that some water penetrates into the polar/apolar interfacial regions of DM-TAP bilayers at temperatures above the $T_m$. However, the fact that the higher-frequency component of the C=O stretching band predominates, leading to a higher overall frequency for the band as a whole, also indicates that the bilayer polar/apolar interfaces of liquid–crystalline DM-TAP bilayers are not as hydrated as those of other phospho- and glyco-glycerolipids.

At low temperatures, the C=O stretching absorption band envelope of DM-TAP seems to be composed predominantly of a fairly narrow component centered near 1747 $cm^{-1}$ and a broader but less intense component centered near 1737 $cm^{-1}$. The sharpness and very high frequency of the higher-frequency component indicate that it arises from a population of highly immobilized ester carbonyl groups that are located in a non-polar environment in which there are no interactions with hydrogen-bonding donor groups [67]. In contrast, the broader, lower-frequency band arises from a population of ester carbonyl groups that are either more mobile and/or are located in a more polar and heterogeneous environment. It is also possible that this latter population may be involved in weak hydrogen-bonding interac-

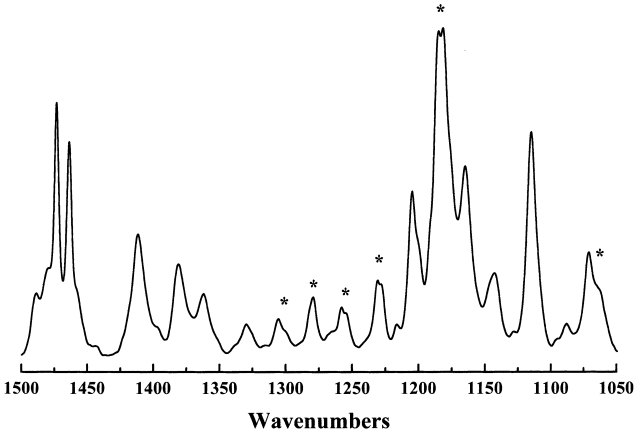


Fig. 6. Absorbance spectra showing the fingerprint region of the infrared spectrum of the $L_c$ phase of DM-TAP. $CH_2$ wagging bands which appear as doublets or two component band envelopes are marked with asterisks. The data shown were acquired at 0°C.

tions with water, since its peak frequency occurs towards the higher end of the range normally expected of hydrogen-bonded ester carbonyl groups. However, this seems unlikely because the frequency of this absorption band (and that of the higher-frequency component) does not change when the $L_c$ phase is formed from dispersions of the lipid in non-deuterated aqueous solvents (data not shown). That the two populations of ester carbonyl groups are essentially insensitive to the effects of H/D exchange also indicates that they are not involved in hydrogen-bonding interactions with the solvent phase. In turn, this suggests that, at low temperatures, water is essentially excluded from the polar/apolar interfacial regions of bilayers composed of this lipid.

The fingerprint region of the infrared spectrum between 1050 and 1500 $cm^{-1}$ reveals other information on the structure and organization of the $L_c$ phase of this lipid. For example, Fig. 6 shows that several of the absorption bands arising from the $CH_2$ wagging band progression appear as either a doublet or a two-component band envelope (see bands marked with asterisks). Given that the $CH_2$ wagging band progression is the result of intrachain vibrational coupling and is essentially independent of interchain interactions [60], this unusual spectroscopic feature may be indicating that the $L_c$ phase of this lipid contains two populations of vibrationally inequivalent all-*trans* polymethylene chains. Also, with most common diacyl glycerolipids, the scissoring vibration of the $\alpha$-$CH_2$ groups on the fatty acyl chains gives rise to a relatively weak absorption band centered near 1410–1420 $cm^{-1}$ (for examples, see [62,63]). However, the relative intensity of the $\alpha$-$CH_2$ scissoring band of DM-TAP is considerably higher than has hitherto been observed. The latter observation provides important information on the conformation of the 1,2-dihydro-3-*N,N,N*-trimethyl aminopropane moiety in the $L_c$ phase of DM-TAP and will be explored further in Section 4.

### 3.3. X-ray diffraction

Further insights into the structural properties of the high- and low-temperature phases of DM-TAP were obtained by an examination of low- and wide-angle X-ray scattering data acquired with both capillary-mounted dispersions and macroscopically oriented samples. The two types of preparations exhibited qualitatively similar data under all conditions examined. The X-ray data obtained from unoriented, capillary-mounted samples of DM-TAP are shown in Fig. 7. The trace acquired at 0°C shows low-angle peaks for diffraction orders $h = 1$, 2 and 4 in the region $q < 0.6$, peaks that index to a lamellar $D$ spacing of 49 Å. With unoriented samples, these peaks are obscured in scans acquired near 25°C, but are clearly resolved in both low-resolution (rotating anode generator) and high-resolution (synchrotron) scans obtained with the oriented samples (data not shown). The high-resolution scans (oriented sample, $T \leq 10$°C) also exhibit an additional low-angle peak for diffraction order $h = 3$ (data not shown).

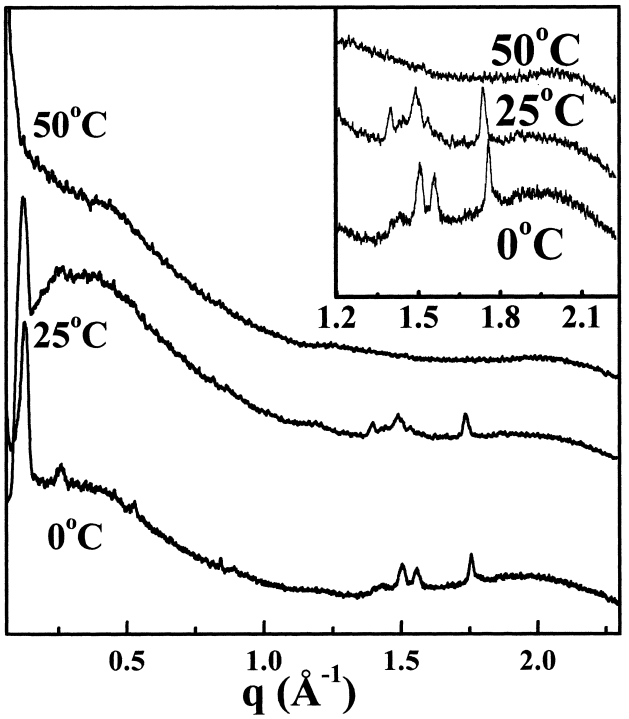


Fig. 7. Low- and wide-angle X-ray diffraction intensity plotted as a function of scattering vector ($q$) along the normal to the bilayers. The data shown are low-resolution scans (rotating anode generator) obtained with unoriented samples of DM-TAP at the temperatures indicated. The inset shows the wide-angle region on an expanded scale.

The low-resolution data acquired at 50°C do not show any low-angle diffraction peaks consistent with the stacking of lamellar structures (see Fig. 7). However, such diffraction peaks rapidly reappear when the sample is cooled to temperatures below the $T_m$,

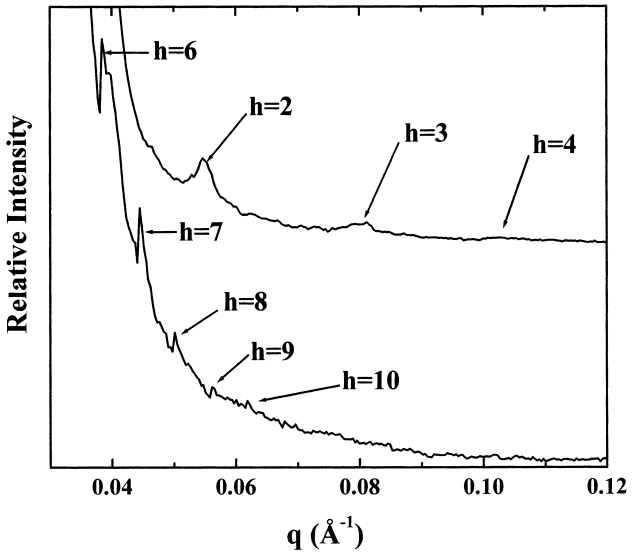


Fig. 8. Low-angle X-ray diffraction intensity plotted as a function of scattering vector ($q$) along the normal to the bilayers. The data shown are high-resolution scans (synchrotron) obtained with an oriented sample of DM-TAP. The sample was close to full hydration in the lower trace and was mildly dehydrated in the upper trace.

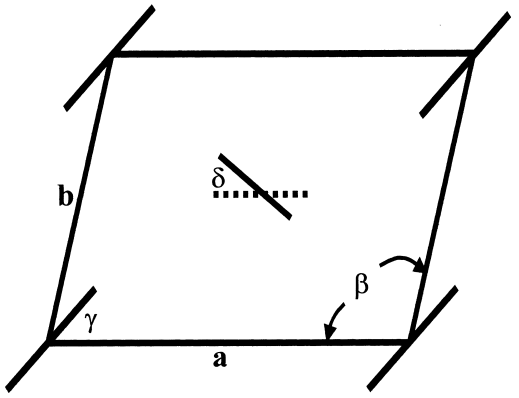


Fig. 9. Schematic representation of the hydrocarbon subcell deduced from X-ray diffraction studies of the $L_c$ phase of DM-TAP. The short lines represent the zigzag of the C–C–C plane of each chain that runs perpendicular to the plane of the paper.

suggesting that complete disruption of bilayer structure did not occur at high temperature. Evidence for lamellar stacking of bilayers at high temperature was also absent in our low-resolution studies of macroscopically oriented samples. However, diffraction peaks were observed at high temperatures in our high-resolution studies of an oriented sample using the much higher intensity of the synchrotron source (see Fig. 8). At temperatures above the $T_m$, the sample yielded rather diffuse diffraction patterns which index to $D$ spacing values $\geq$1000 Å (Fig. 8, lower trace). Upon mild dehydration of the sample, the pattern developed sharper lamellar diffraction peaks consistent with $D$ spacing values near 230 Å (Fig. 8, upper trace). Moreover, under all conditions the diffraction patterns were strongly concentrated on the meridian ($q_z$ axis) as is consistent with the stacking of lipid lamellae. The large $D$ spacings observed can thus be attributed to excessive swelling (so-called 'unbinding') of these charged bilayers at temperatures above $T_m$.

The low-temperature phase of DM-TAP also exhibits three reflections in the wide-angle region (see inset on Fig. 7). These reflections index to the spacings of 3.64, 4.11 and 4.24 Å at 0°C and 3.66 Å, 4.24 Å and 4.56 Å at 25°C which we attribute to the arrangement of the all-*trans* hydrocarbon chains in the unit cell. The sharpness of the peaks is itself consistent with the chains being arranged perpendicular to the bilayer surface (i.e. the hydrocarbon chains are untilted). Also, the absence of many additional peaks suggests that the hydrocarbon chain packing in adjacent bilayers is uncorrelated, as observed with DPPC bilayers [68], thus indicating that the data can be indexed to a two-dimensional unit cell. These data and analyses are similar to those described by Maulik et al. [55] and were used to calculate the area per lipid molecule as well as the unit subcell parameters, and the results are summarized in Table 1 and Fig. 9. In part, the results indicate that the crystalline phase of DM-TAP is a lamellar structure with a $D$ spacing of 48–49 Å,

Table 1
Summary of X-ray structural parameters of the hydrocarbon chain subcell adopted by the low-temperature phase of DM-TAP

| Temperature (°C) | D (Å) | $a$ (Å) | $b$ (Å) | $\beta$ (°) | Area/lipid (Å$^2$) |
|---|---|---|---|---|---|
| 0 | 49 | 7.3 | 5.1 | 92 | 37 |
| 25 | 48 | 7.3 | 5.5 | 94 | 40 |

and that the hydrocarbon chains are arranged in a compact hydrocarbon subcell in which the $\beta$ angle between the *a* and *b* vectors is between 92 and 94°.

Finally, we note that if one assumes that the hydrocarbon chains are untilted, then multiplication of molecular area *A* listed in Table 1 by one half of the *D* spacing value would return a volume estimate ($\cong$916 Å$^3$ at 10°C) representing the mean volume occupied by a single DM-TAP molecule and the average number of bound and interlamellar water molecules associated with it. Using neutral buoyancy methods, we measure a specific volume for the DM-TAP molecule at 10°C of approximately 917 Å$^3$, a value remarkably similar to that calculated from our X-ray diffraction measurements. However, when one considers that the specific volume values returned by the neutral buoyancy methodology do not include contributions from hydration or other associated water molecules [69], it becomes apparent that there must be very little water associated with the DM-TAP molecules in the low-temperature phase. This observation implies that the low-temperature phase of DM-TAP must be a substantially dehydrated structure, in marked contrast to the $L_\alpha$ phase, which swells continuously by imbibing water between the bilayers.

## 4. Discussion

This work provides valuable insights into the thermotropic phase behavior, structure and organization of bilayer membranes derived from the cationic lipid DM-TAP. It is clear that the single phase transition observed upon heating aqueous dispersions of this lipid is not a simple $L_\beta/L_\alpha$-type gel/liquid–crystalline phase transition as is commonly exhibited by many of the naturally occurring classes of glyco- and phospho-glycerolipids. This conclusion is supported by the unusually high enthalpy change associated with this transition ($\cong$15 kcal/mol), a value which greatly exceeds the range ($\cong$5–6 kcal/mol) of the $L_\beta/L_\alpha$ phase transitions of aqueous dispersions of 1,2-diacylphospho- and glycolipid bilayers of comparable hydrocarbon chain length (for examples, see [58,59,70–72]). Our spectroscopic and X-ray diffraction data provide very strong evidence that the observed heating endothermic phase transition involves a direct conversion from a highly ordered and substantially dehydrated crystal-like structure to a hydrated $L_\alpha$ phase (i.e. an $L_c \rightarrow L_\alpha$ phase transition). Thus, in addition to the energy attributable to the conformational melting of the lipid hydrocarbon chains, the observed enthalpy change also includes contributions from the heat of hydration of the headgroup and polar/apolar interfacial moieties, as well as the energy required to break down the highly ordered crystal structure which this lipid forms at low temperatures. Comparable phenomena have been observed with members of several classes of phospho and glyco-glycerolipids (for examples, see [58,59,71–73]) and, as observed with DM-TAP, the low-temperature crystal-like phases of such lipids are highly ordered lamellar structures in which the polar headgroup and/or polar/apolar interfacial regions are partially or substantially dehydrated (for examples, see [58,59,64]).

The FTIR spectroscopic data clearly indicate that the $L_c$ phase is a very highly ordered, substantially dehydrated structure in which highly immobilized hydrocarbon chains are packed with their zigzag planes perpendicular to each other. Of all theoretically feasible modes of hydrocarbon subcell packing (see [74,75]), relatively few have actually been observed in practice [76], and of those, the orthorhombic $\perp$ form is the most commonly observed packing format which is compatible with our spectroscopic observations. Here, because of the extraordinarily high resolution of the FTIR spectroscopic data, one can obtain fairly accurate estimates of the relative intensities of the two components of the $CH_2$ scissoring band and use them to obtain additional information on the alignment between the zigzag plane of the hydrocarbon chain and the *a* axis of the unit cell (for details, see [60]). Our estimates of the relative intensities of the components of the $CH_2$ scissoring band ($I_{1463}/I_{1472}$ ratio $\cong$0.87) suggest that the hydrocarbon chains of the crystalline phase of DM-TAP are arranged in a somewhat distorted orthorhombic $\perp$ subcell in which the zigzag planes of the hydrocarbon chains are rotated by about 4° relative to the 45° angle which is the ideal for orthorhombic $\perp$ packing (see Fig. 9).

The intensity of the infrared absorption band arising from the scissoring vibration of the $\alpha$-$CH_2$ groups is considerably greater than normally ob-

served with naturally occurring phospho- and glycoglycerolipids, where this band is believed to arise predominantly from the scissoring vibrations of α-$CH_2$ groups on *sn*1-fatty acyl chains [77], presumably because of the conformational inequivalence of *sn*1- and *sn*2-α-$CH_2$ groups (for details on the conformations of glycerolipid α-$CH_2$ groups, see [78–82]). The unusually high intensity of the α-$CH_2$ absorption band of DM-TAP suggests that the α-$CH_2$ absorption band of DM-TAP could be a summation of contributions from the α-$CH_2$ groups of both hydrocarbon chains. Alternatively, the enhanced intensity of the α-$CH_2$ scissoring vibration may result from an alignment of the α-$CH_2$ groups of DM-TAP such that their $CH_2$ scissoring vibration could couple with the vibrations of nearby oscillators. It is not clear which of these two mechanisms applies to the $L_c$ phase of DM-TAP. Interestingly, however, these mechanisms both require that the conformations of the α-$CH_2$ groups of DM-TAP are different from that observed in the typical 1,2-diacylglycerolipids. This suggests that the conformation of the 1,2-oxy-3-*N,N,N*-trimethyl aminopropane moiety in the $L_c$ phase of DM-TAP may not be comparable to that adopted by the glycerol backbones of most other classes of 1,2-diacylglycerolipids. Finally, we note that our FTIR spectroscopic data also suggest that there are two vibrationally inequivalent populations of ester carbonyl groups, and two vibrationally inequivalent populations of all-*trans* polymethylene chains, in the $L_c$ phase of DM-TAP, suggesting either inequivalence of the two fatty acyl chains and/or the formation of crystal lattices in which there are at least two inequivalent DM-TAP molecules in the unit cell. It is also not clear which of these two possibilities applies to DM-TAP.

Although the low-temperature phase of DM-TAP is highly crystalline, this molecule poses special difficulties for X-ray diffraction work because its polar headgroup does not contain strongly contrasting electron-dense atoms. Consequently, there were not enough orders of low-angle diffraction to enable the construction of two-dimensional electron density profiles, the availability of which would have enabled more precise calculations of bilayer thickness within the unit cell. Also, DM-TAP headgroups do not have sufficient electron density contrast to allow observation of weak peaks in the intermediate-angle region, data which encode information on the lateral spacing of the polar headgroups [83]. Nevertheless, sufficient information was available from the pattern of wide-angle reflections to enable a reasonably accurate description of the type and dimensions of the hydrocarbon chain subcell. Interestingly, the structural parameters calculated indicate that the hydrocarbon subcell is more accurately defined as a form of monoclinic packing which does not fit neatly into any of the theoretically calculated subcells (for further discussion of the latter, see [75,76]). However, the data could also be interpreted in terms of a distorted orthorhombic subcell in which the *a* and *b* vectors are not quite orthogonal. In an ideal orthorhombic subcell, the *a* and *b* vectors are orthogonal and this would give rise to two wide-angle diffraction peaks corresponding to the (2,0) and (1,1) reflections. With a slight 'distortion' of the $\beta$ angle from 90° (note that our calculated values for $\beta$ are 92 and 94°C), the (11) reflection splits into two components (the (1,1) and $(1,\bar{1})$ reflections) and, as observed experimentally, three wide-angle reflections result. The 'distorted orthorhombic subcell' defined by the X-ray diffraction measurements is also compatible with the FTIR spectroscopic data, which also suggest an orthorhombic subcell in which the angle between the zigzag planes of the hydrocarbon chains and is distorted by some 4° from its ideal value, 45°. This could be easily achieved by a small distortion of the $\beta$ angle away from the orthogonal ideal.

The X-ray data obtained using the high intensity CHESS source clearly indicate that in the presence of excess water, the $L_\alpha$ phase of DM-TAP consists of stacks of bilayers which swell excessively by continuously imbibing water between the bilayers. This so-called 'unbinding' is typical of charged bilayers (for examples, see [84,85]), for which electrostatic repulsion between the bilayers is probably strong enough to cause unbinding of stacks of lipid lamellae [54,86–88]. In contrast, the crystalline phase of DM-TAP consists of strongly bound lamellae with little or no water in the interlamellar spaces. Presumably, this is the result of specific interactions between the headgroups on adjacent bilayers. Such interactions may involve the formation of compact structures in which the positively charged quaternary amino headgroups are bridged by a network of lateral and interlamellar ionic interactions with chloride counterions, such as

observed in crystalline choline chloride [89]. To understand the basis of the conversion of such a strongly bound system to an essentially unbound system upon hydrocarbon chain-melting, one should note that the bending modulus of a lipid bilayer decreases substantially when its hydrocarbon chains melt [90], and as a result, repulsive undulation interactions between the lipid lamellae increase substantially when their gel or quasi-crystalline phases convert to the liquid–crystalline state [91]. This phase state-induced increase in repulsive undulation interactions is one of the driving forces favoring the swelling of aqueous interlamellar spaces at the gel to liquid–crystalline phase transitions of all hydrated lipid bilayers. With bilayers such as DM-TAP, the increased undulation repulsive interaction at the lipid $T_m$ is probably accompanied by weakening the ionic bridges between the charged headgroups and their counterions, and this process will further favor the penetration of water into the interlamellar spaces and concomitant hydration of the charged lipid headgroups and their counterions. The latter process will eventually uncouple the binding of the lipid lamellae and once this occurs, the combination of electrostatic and undulation repulsion will accelerate the swelling of the aqueous interlamellar spaces that ultimately result in unbinding. When compared to neutral lipids, the extreme difference in water spacing between the crystalline and the $L_\alpha$ phases of DM-TAP can thus be attributed to the strong electrostatic repulsion component which emerges in DM-TAP dispersions when the network of bridging counterions is disrupted at the $T_m$ of the lipid. This behavior is different from that exhibited by cationic lipid bilayers composed of dihexadecyldimethylammonium acetate, which unbind in excess water at temperatures above and below the hydrocarbon chain-melting phase transition [86].

The spectroscopic, X-ray diffraction and neutral buoyancy density data all indicate that DM-TAP molecules are essentially dehydrated in the $L_c$ phase and our spectroscopic data suggest that the polar/apolar interfaces of liquid–crystalline bilayers of this lipid are also relatively poorly hydrated. This latter result might appear to contradict the X-ray diffraction data which show that the water spacing between bilayers becomes very large in the liquid–crystalline phase, indicating that the number of water molecules per lipid ($n_w$) must be large. However, one should note that the relevant infrared spectroscopic observations are not a reflection of $n_w$, but $n_{w'}$, the number of water molecules in the interfacial region. That these bilayers have relatively low $n_{w'}$ values can probably be attributed, in part, to the small size of the DM-TAP headgroup, which may facilitate tighter interfacial packing because of decreased steric crowding, and/or the limited capacity of the polar headgroup for interaction with the carbonyl ester groups in the bilayer polar/apolar interfacial region. Such properties may also explain why DM-TAP membranes are less amenable to penetration by membrane-active peptides such as gramicidin S [92]. Currently, it is not clear whether any of the structural differences between this cationic bilayer and most naturally occurring classes of membrane lipids, aside from differences in membrane surface charge, are relevant to its capacity to effect DNA transfection. Further in-depth studies of the physical properties of a wider range cationic lipids should provide greater insights into this particular issue.

## Acknowledgements

The authors would like to thank Dr. John Katsaras for the use of the Chalk River Laboratories X-ray chamber and Dr. Ernie Fontes for assistance in the studies performed at CHESS (supported by NSF Grant DMR-931172). This work was supported by operating and major equipment grants from the Medical Research Council of Canada (R.N.M.), by major equipment grants from the Alberta Heritage Foundation for Medical Research (R.N.M.), and by National Institutes of Health Grant GM44976 (S.T.N., J.F.N.).

## References

[1] T. Kunitake, Y. Okakata, J. Am. Chem. Soc. 9 (1977) 3860–3861.
[2] H. Kunieda, Nippon Kagaku Kaishi (1977) 151–156.
[3] T. Kunitake, Chem. Lett. (1979) 645–648.
[4] Y.Y. Lim, J.H. Fendler, J. Am. Chem. Soc. 101 (1979) 4023–4029.
[5] K. Kano, A. Romero, B. Djermouri, H.J. Ache, J.H. Fendler, J. Am. Chem. Soc. 101 (1979) 4030–4037.

[6] J.H. Fendler, Acc. Chem. Res. 13 (1980) 7–13.
[7] J.L. Parker, Prog. Surf. Sci. 47 (1994) 205–271.
[8] T. Kunitake, Angew. Chem. Int. Ed. Engl. 31 (1992) 709–726.
[9] S. Bhattacharya, M. Subramanian, U.S. Hiremath, Chem. Phys. Lipids 78 (1995) 177–188.
[10] R.C. Ahuja, B.J. Dringenberg, Langmuir 11 (1995) 1515–1523.
[11] Y. Okahata, R. Ando, T. Kunitake, Bull. Chem. Soc. Jpn. 52 (1979) 3647–3653.
[12] P. Scrimm, P. Tecilla, U. Tonellato, J. Am. Chem. Soc. 114 (1992) 5086–5092.
[13] A. Kanazawa, T. Ieda, T. Endo, Antimicrob. Agents Chemother. 38 (1994) 945–952.
[14] M.C. Filion, N.C. Phillips, Br. J. Pharmacol. 122 (1997) 551–557.
[15] K. Ijiro, Y. Okahata, J. Chem Soc. Chem. Commun. (1992) 1339–1341.
[16] P.L. Felgner, Y.J. Tsai, L. Sukhu, C.J. Wheeler, M. Manthorpe, J. Marshall, S.H. Cheng, Ann. N.Y. Acad. Sci. 772 (1995) 126–139.
[17] M. Cotton, E. Wagner, Curr. Opin. Biotech. 4 (1993) 705–710.
[18] I.D. Konstantinova, G.A. Serebrinnikova, Uspejhi Khimi 65 (1996) 581–598.
[19] I.D. Konstantinova, N.I. Zaitseva, I.P. Ushakova, G.A. Serebrennikova, Russ. Chem. Bull. 43 (1994) 1731–1735.
[20] M.J. Bennett, M.H. Nantz, R.P. Balasubramaniam, D.C. Gruenert, R.W. Malone, Biosci. Rep. 15 (1995) 47–53.
[21] A. Zimmer, S.A. Aziz, M. Gilbert, D. Werner, C.R. Noe, Eur. J. Pharm. Biopharm. 47 (1999) 175–178.
[22] T. Akao, T. Fukumoto, H. Ihara, A. Ito, FEBS Lett. 391 (1996) 215–218.
[23] S.J. Eastman, C. Siegel, J. Tousignant, A.E. Smith, S.H. Cheng, R.K. Scheule, Biochim. Biophys. Acta 1325 (1997) 41–62.
[24] I. Koltover, T. Salditt, C.R. Safinya, Biophys. J. 77 (1999) 915–924.
[25] I. Koltover, T. Salditt, J.O. Rädler, C.R. Safinya, Science 281 (1998) 78–81.
[26] R. Zantl, F. Artzner, G. Rapp, J.O. Rädler, Europhys. Lett. 45 (1998) 90–96.
[27] T. Salditt, I. Koltover, J.O. Radler, C.R. Safinya, Phys. Rev. Lett. 79 (1997) 2582–2585.
[28] T. Salditt, I. Koltover, J.O. Radler, C.R. Safinya, Phys. Rev. E 58 (1998) 889–904.
[29] R.P. Balasubramaniam, M.J. Bennett, A.M. Aberle, J.G. Malone, M.H. Nantz, R.W. Malone, Gene Ther. 3 (1996) 163–172.
[30] C. Jiang, S.P. O'Connor, S.L. Fang, K.X. Wang, I.J. Marshal, J.L. Williams, B. Wilburn, Y. Echelard, S.H. Cheng, Hum. Gene Ther. 9 (1998) 1531–1542.
[31] E.R. Lee, J. Marshall, C.S. Siegel, C. Jiang, N.S. Yew, M.R. Nichols, J.B. Nietupski, R.J. Ziegler, M.B. Lane, K.X. Wang, N.C. Wan, R.K. Scheule, D.J. Harris, A.E. Smith, S.H. Cheng, Hum. Gene Ther. 7 (1996) 1701–1717.
[32] M.J. Bennett, A.M. Aberle, R.P. Balasubramaniam, J.G. Malone, R.W. Malone, M.H. Nantz, J. Med. Chem. 40 (1997) 4069–4078.
[33] M.H. Nantz, L. Li, J. Zhu, K.L. Aho-Sharon, D. Lim, K.L. Erickson, Biochim. Biophys. Acta 1394 (1998) 219–223.
[34] K. Kano, A. Romero, B. Djermouri, H.J. Ache, J.H. Fendler, J. Am. Chem. Soc. 101 (1979) 4030–4037.
[35] T. Kunitake, R. Ando, Y. Ishikawa, Mem. Fac. Eng. Kyushu Univ. 46 (1986) 221–243.
[36] T. Kunitake, R. Ando, Y. Ishikawa, Mem. Fac. Eng. Kyushu Univ. 46 (1986) 245–263.
[37] Y. Okahata, R. Ando, T. Kunitake, Ber. Bunsenges. Phys. Chem. 85 (1981) 789–798.
[38] L. Stamatatos, R. Leventis, M.J. Zuckerman, J.R. Silvius, Biochemistry 27 (1988) 3917–3925.
[39] J.R. Silvius, Biochim. Biophys. Acta 1070 (1991) 51–59.
[40] G.G. Mao, Y.H. Tsao, M. Tirrell, H.T. Davis, V. Hessel, H. Ringsdorf, Langmuir 11 (1995) 942–952.
[41] F.M. Linseisen, S. Bayer, T.M. Bayer, Chem. Phys. Lipids 83 (1996) 9–23.
[42] J. Seelig, P.M. MacDonald, P.G. Scherer, Biochemistry 26 (1987) 7535–7541.
[43] P.G. Scherer, J. Seelig, Biochemistry 28 (1989) 7720–7728.
[44] P. Mitrakos, P.M. MacDonald, Biochemistry 35 (1996) 16714–16722.
[45] P. Mitrakos, P.M. MacDonald, Biochemistry 36 (1997) 13646–13656.
[46] R.N.A.H. Lewis, R.N. McElhaney, Biophys. J. 79 (2000) 1455–1464.
[47] S.L. Holmen, M.W. Vanbrocklin, R.R. Eversole, S.R. Stapleton, L.C. Ginsberg, In-Vitro Cell. Dev. Biol. Anim. 31 (1995) 347–351.
[48] T. Stegmann, J.Y. Legendre, Biochim. Biophys. Acta 1325 (1997) 71–79.
[49] R. Wattiaux, M. Jadot, M.T. Warnier-Pirotte, S. Wattiaux-De Coninck, FEBS Lett. 417 (1997) 199–202.
[50] B.D. Friemark, H.P. Blezinger, V.J. Florak, J.L. Nordstrom, S.D. Long, D.S. Deshpande, S. Nochunson, P.L. Petrak, J. Immunol. 160 (1998) 4580–4586.
[51] H.H. Mantsch, C. Madec, R.N.A.H. Lewis, R.N. McElhaney, Biochemistry 24 (1985) 2440–2446.
[52] S. Tristram-Nagle, R. Zhang, R.M. Suter, C.R. Worthington, W.-J. Sun, J.F. Nagle, Biophys. J. 64 (1993) 1097–1109.
[53] J. Katsaras, S. Tristram-Nagle, Y. Liu, R.L. Headrick, E. Fontes, P.C. Mason, J.F. Nagle, Phys. Rev. E 61 (2000) 5668–5677.
[54] M.W. Tate, E.F. Eikenberry, S.O. Barna, M.E. Wall, J.L. Lowrance, S.M. Gruner, J. Appl. Cryst. 28 (1995) 196–205.
[55] P.R. Maulik, M.J. Ruocco, G.G. Shipley, Chem. Phys. Lipids 56 (1990) 123–133.
[56] R.N.A.H. Lewis, R.N. McElhaney, in: H.H. Mantsch, D. Chapman (Eds.), Infrared Spectroscopy of Biomolecules, Wiley-Liss, NY, 1996, pp. 159–202.
[57] R.G. Snyder, J. Chem. Phys. 47 (1967) 1316–1360.
[58] R.N.A.H. Lewis, R.N. McElhaney, Biophys. J. 64 (1993) 1081–1096.

[59] Y.-P. Zhang, R.N.A.H. Lewis, R.N. McElhaney, Biophys. J. 72 (1997) 779–793.
[60] R.G. Snyder, J. Mol. Spectrosc. 7 (1961) 116–144.
[61] R.G. Snyder, J. Chem. Phys. 71 (1979) 3229–3235.
[62] R.N.A.H. Lewis, R.N. McElhaney, Biochemistry 29 (1990) 7946–7953.
[63] R.N.A.H. Lewis, R.N. McElhaney, Biophys. J. 61 (1992) 63–77.
[64] R.N.A.H. Lewis, D.A. Mannock, R.N. McElhaney, P.T.T. Wong, H.H. Mantsch, Biochemistry 29 (1990) 8933–8943.
[65] A. Blume, W. Hübner, G. Messner, Biochemistry 27 (1988) 8239–8249.
[66] R.N.A.H. Lewis, R.N. McElhaney, W. Pohle, H.H. Mantsch, Biophys. J. 67 (1994) 2367–2375.
[67] E.C. Mushayakarara, P.T.T. Wong, H.H. Mantsch, Biochem. Biophy. Res. Commun. 134 (1986) 140–145.
[68] W.J. Sun, R.M. Suter, M.A. Knewtson, C.R. Worthington, S. Tristram-Nagle, R. Zhang, J.F. Nagle, Phys. Rev. E 49 (1994) 4665–4676.
[69] M.C. Wiener, S. Tristram-Nagle, D.A. Wilkinson, L.E. Campbell, J.F. Nagle, Biochim. Biophys. Acta 938 (1988) 135–142.
[70] R.N.A.H. Lewis, N. Mak, R.N. McElhaney, Biochemistry 26 (1987) 6118–6126.
[71] D.A. Mannock, R.N.A.H. Lewis, R.N. McElhaney, Biochemistry 29 (1990) 7790–7799.
[72] D.A. Mannock, R.N.A.H. Lewis, A. Sen, R.N. McElhaney, Biochemistry 27 (1988) 6852–6859.
[73] M. Kodama, T. Miyata, T. Yokoyama, Biochim. Biophys. Acta 1168 (1993) 243–248.
[74] A.I. Kitaigorodskii (1961) Organic Chemical Crystallography, Organic Consultants Bureau, New York (authorized translation from Russian).
[75] E. Segerman, Acta Cryst. 19 (1965) 789–796.
[76] S. Abrahamsson, B. Dahlén, H. Löfgren, I. Pascher, Prog. Chem. Fats Lipids 16 (1978) 125–143.
[77] R.N.A.H. Lewis, W. Pohle, R.N. McElhaney, Biophys. J. 70 (1996) 2736–2746.
[78] G. Buldt, H.U. Gally, J. Seelig, G. Zaccai, J. Mol. Biol. 134 (1979) 673–691.
[79] H. Hauser, I. Pascher, S. Sundell, Biochemistry 27 (1988) 9166–9174.
[80] H. Hauser, I. Pascher, R.H. Pearson, S. Sundell, Biochim. Biophys. Acta 650 (1981) 21–51.
[81] P.B. Hitchcock, R. Mason, K.M. Thomas, G.G. Shipley, Proc. Natl. Acad. Sci. USA 71 (1974) 3036–3040.
[82] R.H. Pearson, I. Pascher, Nature (London) 281 (1979) 499–501.
[83] J. Katsaras, V.A. Raghunathan, E.J. Dufourcq, J. Dufourcq, Biochemistry 34 (1995) 4684–4688.
[84] H. Hauser, Biochim. Biophys. Acta 772 (1984) 32–50.
[85] R.D. Koynova, B.G. Tenchov, H. Kuttenreich, H.-J. Hinz, Biochemistry 32 (1993) 12437–12445.
[86] Y. Tsao, D.F. Evans, R.P. Rand, V.A. Parsegian, Langmuir 9 (1993) 233–241.
[87] M.E. Loosley-Millman, R.P. Rand, V.A. Parsegian, Biophys. J. 40 (1982) 221–232.
[88] T.J. McIntosh, S.A. Simon, Biochemistry 33 (1994) 10477–10486.
[89] M.E. Senko, D.H. Templeton, Acta Cryst. 13 (1960) 281–285.
[90] T.J. McIntosh, S.A. Simon, Biochemistry 32 (1993) 8374–8384.
[91] W. Helfrich, Z. Natforsch. 33a (1978) 305–315.
[92] R.N.A.H. Lewis, E.J. Prenner, L.H. Kondejewski, C.R. Flach, R. Mendelsohn, R.S. Hodges, R.N. McElhaney, Biochemistry 38 (1999) 15193–15203.